When things add up: environmental structure and microbial interactions drive antibiotic resistance plasmid evolution

Laurens E. Zandbergen[1], Mishelle Bustamante[1], Jan-Maarten Luursema[2], Thomas Hackl[1], Marjon G.J. de Vos[1*]

1 Groningen Institute of Evolutionary Life Sciences (GELIFES), University of Groningen, Groningen, The Netherlands

2 Radboud University Medical Center, Nijmegen, the Netherlands

*corresponding author: m.g.j.de.vos@rug.nl

Competing interests

The authors declare no conflict of interest.

Abstract

Background and objectives:

Antimicrobial resistance is a major global health threat, driven in part by the rapid evolution of resistance in pathogens, which undermines the effectiveness of antimicrobial treatment. In infections, pathogens rarely live in a well-mixed, single species environment. It is an open question how microbial interactions in contrasting environmental structures affect plasmid mediated antibiotic resistance evolution.

Methodology:

This study investigates how a spatially structured versus a well-mixed liquid environment, together with microbial interactions, affect antibiotic resistance evolution in uropathogenic *Escherichia coli.* We conducted a serial transfer experiment under increasing concentrations of trimethoprim-sulfamethoxazole comparing resistance evolution in the well-mixed and spatially structured environments, both in the presence and absence of a polymicrobial community.

Results:

Our results revealed that *E. coli* in community context displayed parallel evolutionary trajectories, leading to higher final antibiotic tolerance, while the spatial structure allowed for prolonged resistance evolution. Copy number variation of the plasmid-borne resistance locus varied significantly across conditions; *E. coli* evolved in the well-mixed, monoculture conditions, exhibited the greatest increases in copy number, whereas lineages evolved in the presence of the community showed minimal changes relative to the ancestor.

Conclusions and implications:

These findings underscore the complex interplay between the genetic basis of resistance, the environmental structure and microbial ecology in shaping plasmid-mediated antimicrobial resistance evolution.

Lay summary

Antibiotic resistance depends on environmental context, microbial interactions, and genetics. This study shows that *E. coli* evolved resistance differently in mixed versus structured environments, with changes in plasmid-borne resistance gene copy number. Community interactions led to similar evolutionary paths and higher tolerance, while well-mixed, single-species conditions drove larger genetic changes.

Main Text

Background and objectives

Polymicrobial communities can have a profound effect on the severity of infections[1–4] and can diminish treatment efficacy of pathogens.[5–8] Pathogens are increasingly becoming resistant to antimicrobials, complicating treatments.[9] According to the World Health Organization, antimicrobial resistance (AMR) is among the top ten of threats to global health.[10]

Emerging research shows that AMR can be a collective trait that develops within bacterial communities.[7,11,12] For example, tolerance to antibiotics can be increased in a community by decreasing antibiotic pressures in the local environment through antibiotic degradation, leading to increased pathogen density.[13–15] Higher population densities have been shown to decrease the susceptibility to certain antibiotics, a phenomenon known as the inoculum effect.[16,17] Additionally, microbial communities are often driven by competitive interactions, which lead to a reduction in population size per community member and therefore a change in survival.[18] Yet, cooperation also occurs, particularly in stressful environments[19,20], and it has been observed that interspecies interactions can lead to antibiotic protective effects.[11,21,22]

The environmental structure of bacterial communities can have a large impact on bacterial growth. Virtually all known bacteria are capable of forming biofilms or attaching to surfaces, which, through differences in lifestyle enhances their tolerance to environmental stressors, both biotic and abiotic.[23,24] Surface attached spatial growth versus planktonic lifestyle in a well-mixed environment has different effects on the selective pressures and growth of bacterial populations, such as alterations in competitive and mutualism dynamics.[25,26] Environmental structure has been implicated as a critical factor for the stability and coexistence of species in a community.[27–29] For example, gene expression related to quorum sensing, and consequently antibiotic susceptibility,[22,30] is different in a spatially structured environment compared to a well-mixed environment.[31] Importantly, theorical and empirical research suggests that social interactions of bacteria in spatially structured environments are significantly altered compared to environments with better mixing, leading to different survival outcomes.[32–35]

Environmental structure and microbial lifestyle can influence ecological interactions among microbes. Such different ecological interactions can in turn affect microbial co-existence and evolution.[27–29] Previous studies indicated that populations in spatially structured environments adapt more slowly than those in well-mixed environments [25,36–38], as evolution in a spatially

structured environments increases genetic drift and founder effects in local populations reducing the rate of adaptation.[25,38] Additionally, mixed environments typically lead to a decrease of metabolite exchange among species, focal species will therefore potentially be less affected by the presence of community members.[39,40]

Antimicrobial resistance is often conferred by plasmids containing antibiotic resistance genes. Microbial lifestyle, environmental and community context influence the emergence of plasmid encoded resistance[41–44]. It is unclear how these factors affect the repeatability of plasmid acquired antibiotic resistance evolution. We therefore investigate the effect of the presence and absence of a four-member microbial community of a focal pathogenic species, in two contrasting environments, a well-mixed liquid and a spatially structured solid-surface environment on the repeatability of antibiotic resistance evolution.

Materials and methods

Bacterial isolates and growth medium

The focal *Escherichia coli* isolate and three community isolates (*Klebsiella pneumoniae*, *Enterococcus faecium*, and *Staphylococcus epidermidis*) were collected anonymously in a previous study from elderly patients (>70 years old) who were suffering from a urinary tract infection.[45] The three community members were picked based on their ability to grow in Lysogeny Broth (LB) containing 250 µg/mL trimethoprim and 1250 µg/mL sulfamethoxazole, and being able to clearly distinguish all four isolates on CHROMagar Orientation (CHROMagar). The *E. coli* isolate was selected based on its sensitivity to trimethoprim/sulfamethoxazole. Pure cultures of each separate isolate were obtained by streaking on CHROMagar plates, selecting a single colony, and growing overnight in LB broth at 37°C. Overnight cultures were used to create glycerol stocks (25% glycerol v/v) which were subsequently stored at -80°C. The experiments were performed in Artificial Urine Medium (AUM), which is created (for a 1X concentration) by mixing 1.5 g/L bacto peptone L37 (BD), 3.15 g/L NaHCO3, 11.25 g/L urea (Roth), 4.8 g/L Na2SO4.10H2O, 1.8 g/L K2HPO4, 1.95 g/L NH4Cl, 15 mg/L bacto yeast extract (BD), 1.98 mM lactic acid (Roth), 600 mg/L citric acid, 105 mg/L uric acid, 1.2 g/L creatinine, 4.44 mg/L CaCl2.2H2O, 1.8 g/L Fe(II)SO4.7H2O (Riedel), 368 mg/L MgSO4.7H2O, 1.43 g/L KH2PO4, 5.1 g/L NaCl. Chemicals were ordered from Sigma, unless stated otherwise. The pH was adjusted to 6.5 using 1M HCl.

Antibiotic and X-gal stocks

The trimethoprim stock was created by mixing 10 mg/mL trimethoprim in dimethyl sulfoxide (DMSO), and the sulfamethoxazole stock was created by mixing 50 mg/mL sulfamethoxazole in acetone. The X-gal stock contained 20 mg/mL X-Gal and 0.1M Isopropyl β-D-1-thiogalactopyranoside (IPTG) mixed in DMSO. Both antibiotics, the X-gal, IPTG and solvents were ordered from Sigma. The trimethoprim stock was stored at 4°C for up to two weeks, and the X-gal stock and sulfamethoxazole stocks were stored at -20°C. Trimethoprim and sulfamethoxazole were always mixed in a 1:5 ratio, similar to clinical settings.[46]

Bacterial hotel creation and transfer protocol

Silicon hotel agar molds were stored in 70% ethanol and were dried in a sterile flow cabinet before pouring agar. Each agar hotel was created by mixing 12.5 mL 2x AUM, an appropriate amount of antibiotics, 12.5 mL 3% soft agar in demineralized water at 60°C, and 125 µL X-Gal stock for the visualization of *E. coli* into the hotel mold. X-Gal makes *E.coli* turn blue. Agar hotels were cooled for 30 minutes before removing the agar from the molds.

Five replicates of *E. coli* were evolved for 60 bi-daily transfers in in isolation and in communities with *K. pneumoniae*, *E. faecium* and *S. epidermidis.* Starting cultures of all isolates were created by growing each separately in 1x AUM overnight at 37°C shaken at 200 rpm. Each culture was diluted a hundred times in 1x AUM. Starting agar hotels were created with the starting antibiotics concentration of 50:250 µg/mL TMP:SMX, this 1:5 ratio was picked to resemble the ratio used in clinical settings.[46] Following the layout of Figure S4, 0.5 µL of each diluted culture was added to the middle of the appropriate well on the agar plate. Added cultures were allowed to dry for five minutes before incubating the agar hotels at 37°C for 48 hours. We did not observe any spillover of colonies to other compartments.

Before transferring *E. coli* to a fresh agar hotel, images of hotels were taken and based on the surface area of the *E.coli* colony, if the colony's growth exceeded 1mm of the starting colony, the concentration of antibiotics would be increased by 20%. Unless the antibiotics concentration was increased during the previous transfer. Exception here were the first two transfers where antibiotics were increased by 20% due to clear overgrowth of *E. coli*. Colonies were transferred by streaking around the outer edges of each *E. coli* colony five times and suspending bacteria in 50 µL of 1x AUM. After mixing, 0.5 µL of each replicate would be added to the fresh agar hotels. Wild type community members (non-*E. coli*) were always added as hundred times diluted overnight culture in 1x AUM to the fresh agar hotels.

Liquid serial transfers protocol

154 *E. coli* was evolved over 120 days in AUM transferring replicates to fresh 5 mL medium every
155 48 hours for 60 transfers in total. To start, the *E. coli* and the three community members were
156 streaked on agar to obtain a pure culture of a single colony that was cultured overnight in AUM
157 at 37°C, shaken at 200 rpm. Isolates were diluted a hundred times by adding 50 µL to 5mL
158 total preheated medium. Five replicates of *E. coli* in isolation and five replicates of *E. coli* with
159 the three community members *K. pneumoniae, E. faecium*, and *S. epidermidis*. An appropriate
160 amount of the antibiotics were added to the medium before adding the bacteria. Antibiotic
161 concentration started at 50:250 µg/mL TMP:SMX, 50% of the *E. coli* minimum inhibitory
162 concentration. Cultures were allowed to grow for 48 hours at 37°C and shaken at 200 rpm.
163 During transfer, the culture was diluted a hundred times and community members were added
164 from stock. Remaining culture was used for obtaining CFU/mL counts for *E. coli* on
165 CHROMagar plates. If *E. coli* had exceeded $1*10^6$ CFU/mL, antibiotic concentration would be
166 increased by 20% for the next transfer. For the first two transfers for *E. coli* evolving in
167 presence of the community, the antibiotic concentration was increased by 20% immediately
168 due to observed high population growth based on turbidity.
169
170 **MIC and MBC assays**
171 Minimal inhibitory concentrations (MIC) of replicates were measured in liquid. Using the
172 concentration of antibiotics at the final transfer step as a guideline, a dilution series was created
173 for each isolate specifically. Measurements were performed in 96-well microtiter plates, using
174 1 x AUM as growth medium. Stationary phase cultures of *E. coli* replicates were used for
175 experiments, diluting them 40x times in the medium antibiotics' mixture. Plates were incubated
176 overnight at 37°C, shaken at 200 rpm. Growth was measured through absorbance at 600nm
177 using a BMG CLARIOstar microplate reader. If the absorbance with the background subtracted
178 exceeded 0.1, it was assumed that *E. coli* had grown using the lowest concentration of
179 antibiotics where no growth was observed is the MIC. All MIC measurements were performed
180 in triplicate.
181
182 Minimal bactericidal concentration (MBC) assays, which can be seen as extended MIC assays
183 in which the community is also present, were performed following the above protocol, but with
184 community members added together with the *E. coli* before overnight growth. After OD600
185 measurements to establish growth in the plate reader, the presence of *E. coli* was established
186 by transferring 1µL using a 96-well pinning tool to CHROMagar, followed by overnight

187 growth at 37°C. The lowest concentration of antibiotics where no growth of *E.coli* was
188 observed on CHROMagar is the MBC.
189
190 **DNA extraction and sequencing**
191 DNA from first transfer clones and final transfer mutants were extracted using the QIAamp
192 DNA Mini Kit (Qiagen, Hilden, Germany) following the manufacturer's instructions. DNA
193 was eluted in 100 µL elution buffer AE. Quality and quantity of isolated DNA were checked
194 using a Nanodrop One^{C} Microvolume UV-Vis Spectrophotometer (Thermo Fisher Scientific,
195 USA).
196 Three clones of the final transfer step for each of the five replicate lineages per experimental
197 setting were sent for illumina sequencing at SeqCenter (Pittsburgh, PA, USA). Five replicates
198 of community members isolated from *E. coli* community agar and liquid were also sent to
199 SeqCenter, Pittsburgh, USA for Illumina sequencing.
200 Illumina sequencing libraries were prepared using the tagmentation-based and PCR-based
201 Illumina DNA Prep kit and custom IDT 10bp unique dual indices (UDI) with a target insert
202 size of 320 bp. No additional DNA fragmentation or size selection steps were performed.
203 Illumina sequencing was performed on an Illumina NovaSeq 6000 sequencer in one or more
204 multiplexed shared-flow-cell runs, producing 2x151bp paired-end reads. Demultiplexing,
205 quality control and adapter trimming was performed with bcl-convert1 (v4.1.5). In total 10.9
206 Gbp and 359.2 Gbp of read data were produced from ancestral and evolved strains,
207 respectively.
208 Ancestor strains were sent to the same company for Nanopore sequencing. Sample libraries
209 were prepared using Oxford Nanopore Technologies (ONT) Ligation Sequencing Kit (SQK-
210 NBD114.24) with NEBNext® Companion Module (E7180L) to manufacturer's specifications.
211 All samples were run on Nanopore R10.4.1 flow cells and MinION Mk1B device. Post-
212 sequencing, Guppy (v6.3.8) was used for super high accuracy base calling (SUP) and
213 demultiplexing. Overall, 2.9 Gbp of read data were produced.
214
215 **Genome assembly, annotation variant calling and effect prediction**
216 The wildtype reference assembly was generated with flye v2.9.2 (settings: --nano-hq)[47] from
217 the ancestral nanopore data and polished using ancestral Illumina read with polca.sh included
218 in the MaSuRCA v4.1.0 Genome Assembly and Analysis Toolkit.[48] Genes were annotated with
219 Bakta v1.8.1[49] and integrated prophages and plasmids with genomad v1.7.4[50] for each replicate
220 were called from read mappings generated with minimap2 v2.26[51] using freebayes v1.3.1

221 (settings: -p 1 -0 -F 0.5)[52] and filtered for spurious calls with bcftools v1.17 (--exclude
222 'REF~"N" || QUAL < 20 || INFO/DP < 10').[53] Variant effects were predicted with the Ensembl
223 Variant Effect Predictor (VEP) v110.1 command line tool.
224
225 ***H*-index calculation**
226 To quantify the repeatability of mutations within our *E. coli* mutants, the *H*-index of genome
227 repeatability previously described by Schenk *et al*. was calculated.[54] The *H*-index was
228 calculated on the functional (COG) and at the gene level. The final *H*-index value falls between
229 0 (no repeated evolution) and 1 (complete parallelism). An *H*-index value of 0.5 indicates that
230 two compared mutants have half of their mutations shared between them.
231
232 **Statistical analysis**
233 When comparing the values between two conditions of mutants, an ANOVA and two-tailed
234 *Welch's t*-test were performed to test the null hypothesis that the two parameters do not have
235 significantly different values (hypothesis of neutrality). To determine level of correlation
236 between two variables, we used the square of a Pearsson correlation coefficient and resulting
237 *P*-value where the null-hypothesis was rejected with a significance level above 0.05. For
238 multiple pairwise comparisons, we used independent sample *t*-tests for all sets with a
239 Bonferroni-correction to adjust *P*-values to reduce type I errors.
240
241 **Results**
242 **Environmental structure and microbial community impact evolutionary trajectories**
243 To study the effects of structure and community context on the evolution of antibiotic
244 resistance, we evolved a uropathogenic isolate of *E. coli* carrying a plasmid encoding resistance
245 genes that only confer low resistance in a serial transfer evolution experiment under four
246 different conditions. Evolving cultures were transferred bi-daily over 120 days, in artificial
247 urine medium (AUM) containing increasing levels of trimethoprim-sulfamethoxazole. In each
248 condition five replicate cultures of *E. coli* were evolved in both a (i) well-mixed and (ii)
249 spatially structured AUM environment, both in the (iii) presence and (iv) absence of a
250 community of three other bacterial species. These other species are often co-isolated with *E.*
251 *coli*; *K. pneumoniae, E. faecium* and *S. epidermidis* in polymicrobial urinary tract infections
252 (Materials and Methods).[45]
253

Phenotypic evolutionary trajectories of *E. coli* across replicate lineages overlapped for three of the four conditions. Replicate lineages overlapped for *E. coli* evolved in the spatially-structured environments in the presence and absence of the community. Replicate lineages of *E. coli* evolved in the well-mixed environment in the presence of the community also overlapped (Figure 1AB), but not in the absence of the community. Thus, the presence of the community leads to the canalization of the phenotypic evolutionary trajectories of *E. coli* in the well-mixed environment (Figure 1B).

For the three overlapping replicate trajectories, the rate of evolution in initial weeks approached the hypothetical maximum rate. For the well-mixed environment, this persisted until day 80, whereas in the spatially structured environment the maximum rate lasted until day 48 for the *E. coli* evolved in presence of the community and until day 30 for *E. coli* evolved in isolation (Figure 1AB). These patterns suggests that within each of these environments, selective pressures drove evolution in a specific direction, potentially funneling evolution towards similar evolutionary outcomes and resulting in convergence of the phenotypic trajectories.

The presence of the community increased the level of antibiotics that *E. coli* can tolerate in both the well-mixed and spatially structured environments (P=0.023 for the community impact in the well-mixed environment and P<0.001 for the community impact in the spatially structured environment, *Welch's t-test*). The final concentration of antibiotics that the evolved *E. coli* populations could sustain were higher in the community context than in isolation in both environments.

In addition to community context, environmental structure, either well-mixed liquid AUM versus spatially structured solid AUM-agar, influenced the evolutionary trajectories of *E. coli*. Initially, the rate of antibiotic increase was identical for both environments. However, after 48 days of evolution (24 transfers) the trajectories began to diverge. In the spatially structured community environment, the rate at which the antibiotic could be increased declined slightly, compared to the well-mixed community environment. Despite this slower rate, *E.coli* evolving at the spatially structured environments tolerated higher concentrations of antibiotics compared to the well-mixed conditions at the final transfer (Figure 1AB). We note that the antibiotic solvents could have influenced adaptation at the end of the experiments when antibiotic concentrations are high. Overall, these results demonstrate that environmental structure differentiated the course of the evolutionary trajectories, with well-mixed liquid and solid-surface environments following distinct evolutionary paths (one-way ANOVA, P<0.001 for liquid versus solid). These results show that both community presence, as well as environment

288 structure had an impact on the evolutionary trajectories of trimethoprim-sulfamethoxazole
289 resistance of *E. coli*. Community context promoted parallelism among evolutionary trajectories
290 and higher final antibiotic tolerance, while spatial structure allowed for prolonged resistance
291 evolution and higher final antibiotic concentrations than those in well-mixed environments.
292
293 **Community interactions mediate response to selection**
294 Uropathogenic *E. coli* is known for its flexible metabolism, enabling it to adapt and respond to
295 fluctuating nutrients in the environment.[55] We investigated whether *E. coli* would respond
296 differently to the presence of antibiotics in a community context. We observed that the focal
297 *E. coli* outgrew the other community members. During the initial 30 days the density of *E. coli*
298 was between the 10^8 and 10^9 CFU/mL for most replicates at the time of transfer in the well-
299 mixed environment in the presence of the community, compared to between 10^6 and 10^7
300 CFU/mL in isolation (Figure 1C, $P<0.001$ for the first 30 days, ANOVA). This high population
301 density in the presence of the community was maintained even after the antibiotic concentration
302 reached the initial MIC at day 12. Even though the community members are highly resistant
303 (>1:5 mg/mL TMP:SMX), *E. coli* achieved higher population densities from the onset of the
304 experiment.
305
306 Similarly, in the spatially structured environment, *E. coli* benefited from the presence of the
307 community; colonies surrounded by the community members were approximately three-fold
308 larger in surface area compared to *E. coli* colonies surrounded only by other *E. coli* colonies
309 (Figure 1D, $P<0.001$ for the difference between community and isolation colonies, *Welch's t-*
310 *test*). Population sizes among the five replicates lineages evolved within the same environment
311 did not differ significantly (Figure 1CD, $P>0.05$, independent samples *t*-test with Bonferroni
312 correction).
313
314 In the well-mixed liquid environment, the presence of the three-species community accelerated
315 the rate at which the antibiotic could be increased in the experiment. When *E.coli* was grown
316 in the presence of the community, *E. coli* lineages surpassed the wild type MIC level after 12
317 days, whereas lineages evolved in isolation required 16-18 days ($P<0.001$, ANOVA). In
318 contrast, in the spatially structured environment, all replicates reached the native MIC after 12
319 days, regardless of whether *E.coli* evolved in the presence or absence of the community and
320 despite the larger colony sizes of *E.coli* in the presence of the community.
321

322 The beneficial effects of the community on *E.coli* population size diminished over time. In the
323 well-mixed environment, the rate of antibiotic increase slowed down after approximately 80
324 days (Figure 1A, dark blue graph). This slow-down occurred simultaneously across all five
325 replicate lineages, which suggests that the community canalizes phenotypic trajectories in a
326 consistent manner. Such a synchronization of the phenotypic evolutionary trajectories was not
327 observed for the replicate lineages of *E. coli* in isolation (Figure 1A, light blue graphs). Some
328 of the replicate lineages of *E.coli* evolving in isolation leveled off much earlier in the
329 experiment, showing a slower phenotypic evolutionary trajectory, with a lower final level of
330 antibiotics. For the spatially structured environment, such a pronounced slow-down and
331 diminishing effect of the community were not observed. The antibiotic concentrations reached
332 at the final transfer were higher for all lineages evolved in the spatially structured solid
333 environment, than for those in the well-mixed environment, both in the presence and absence
334 of the community (Figure 1B).
335
336 Also the population sizes of the community members declined over time. *K. pneumoniae* was
337 initially abundantly present in the well-mixed environment (between 10^7 and 10^8 CFU/mL),
338 but steadily decreased to between 10^6 and 10^7 CFU/mL after 14 days. At later time points, *K.*
339 *pneumoniae* was no longer detected, indicating an abundance at least 100-fold lower than that
340 of *E. coli*, which was below the detection limit. In the spatially structured environment, *K.*
341 *pneumoniae*, steadily decreased in colony size during the first 14 days, consistent with
342 population dynamics in the well-mixed environment. Colony sizes continued to decline with
343 every increase in antibiotic concentration, indicating that rising antibiotic levels affects the
344 wild-type *K. pneumoniae* fitness negatively (average colony size at day 2, 14494 pixels, at day
345 120, 8518 pixels).
346 *E. faecium* was initially present in low numbers (around 10^2 -10^3 CFU/mL), as expected based
347 on previous studies,[4,11] yet population sizes declined with increasing antibiotic concentrations,
348 decreasing by at least five-fold between over the 120 day experiment. *S. epidermidis* was rarely
349 detected during the experiments, indicating population sizes below 10^3 CFU/mL, even though
350 *S. epidermidis* is typically more abundant in isolation (10^4-10^5 CFU/mL). This suggests that
351 competition with other species, or the increasing antibiotics concentrations limited the growth
352 of *S. epidermidis*, even though it can survive high antibiotic concentrations[8]. The decline of
353 both the focal species and community members over time could point to increased competition,
354 reduced cooperation, or a general fitness decrease associated with the rising antibiotic
355 concentration in the environment.

356

357 **Environmental structure and community effect on evolved antibiotic resistance level**

358 Comparing the resistance level of *E. coli* lineages evolved in isolation with the lineages evolved
359 in the presence of the community, we found that the lineages evolved in the well-mixed
360 environment and the spatially structured environment differed. Although lineages evolved in
361 the spatially structured environment tolerated higher concentrations of antibiotics at the end of
362 the experiment than those in the well-mixed environment (Figure 1AB), we find that lineages
363 evolved in the spatially structured environment exhibited lower MICs than those in the well-
364 mixed environment when evolved in the presence of the community (resp. 0.8:4 mg/mL
365 TMP:SMX and 3.2:16 mg/mL TMP:SMX, Figure 2A, Materials and Methods). This
366 discrepancy suggests that different lifestyle (surface or liquid growth) or population dynamics
367 affected antibiotic resistance evolution.

368

369 A similar pattern was observed for *E. coli* evolved in isolation in both environments. In the
370 spatially structured environment, lineages tolerated higher antibiotic concentrations at the final
371 transfer compared to those in the well-mixed environment. However, the MICs of *E. coli*
372 evolved in the spatially structure environment were lower (MIC 0.92:4.6 mg/mL TMP:SMX)
373 than those of three of the five replicates from the well-mixed environment, (MIC 1.06:5.3
374 mg/mL TMP:SMX; $P<0.001$, *Welch's t-test*). The remaining two replicates in the well-mixed
375 environment had a lower MIC (0.27:1.33 and 0.13:0.66 mg/ml TMP:SMX) and corresponded
376 to those lineages that sustained a lower final antibiotic concentration in the evolution
377 experiment (Figure 1A, light blue graphs, Figure 2A).

378

379 Based on the observation that *E.coli* population sizes increased in the presence of community
380 members, we hypothesized that *E. coli* benefited from one or more of the community members
381 during the evolution experiment. To investigate this, we measured the minimum bactericidal
382 concentration (MBC) at which the focal species could no longer be detected when cultured in
383 the presence of the community (Figure 2B, Figure S1, Materials and Methods). We found that
384 *E.coli* lineages evolved in the well-mixed environment in absence of the community could
385 sustain twice the concentration of antibiotics when cultured in the presence of the community
386 (MBC of 1.6:8 mg/mL TMP:SMX for 3 out of 5 replicates), compared to their MIC in isolation
387 (0.8:4 mg/mL TMP:SMX for those same replicates) (Figure S1). In contrast, for lineages
388 evolved in the well-mixed environment in the *presence* of the community, we observed a lower
389 MBC compared to the MIC in presence of the community (MIC of 3.2:16 mg/mL TMP:SMX,

390 MBC 1.6:8 mg/mL TMP:SMX). Indicating that the community negatively affected the growth
391 of *E. coli* lineages that evolved in the presence of that community in the well-mixed
392 environment. Interestingly, *E. coli* lineages evolved in the spatially structured environment
393 benefited from the presence of the community; sustaining a two-fold higher concentration
394 compared to the MIC (Figure 2B). These results indicate that the community generally has a
395 positive effect on antibiotic tolerance of *E. coli* even after resistance evolution, except when *E.*
396 *coli* evolved in the presence of the community in the well-mixed environment.
397
398 **Copy number variation of resistance loci on plasmid**
399 To gain insights into the genetic basis of the evolved antibiotic resistance, we sequenced three
400 clones from the final transfer of each of the five replicate lineages evolved under each condition
401 and compared these sequences to that of the ancestor (Materials and Methods, Table S1). The
402 ancestral strain, despite being highly sensitive to the start concentration of TMP-SMX at the
403 beginning of the experiment, did carry a 138K base pair sized IncFII-plasmid that contains
404 genes annotated to encode for resistance against both antibiotics, *dfrA17* and *sul1*. *DfrA17*
405 confers resistance to trimethoprim, s*ul1* encodes a dihydropteroate synthase, conferring
406 resistance to sulfamethoxazole. These resistance genes are located in an Tn21-like integron
407 cassette, which is similar to a cassette first described by Liebert in 1999 (Figure S2).[56] At the
408 time of the description, the transposon did not yet contain the *dfrA17* gene, or any of the other
409 resistance genes located on that cassette.
410
411 We assessed the plasmid copy numbers in the evolved clones and in the ancestor. The *E. coli*
412 ancestor contained two copies of the plasmid relative to the host chromosome (Figure 3A). The
413 evolved lineages had a similar plasmid copy number, indicating that plasmid copy number
414 could not explain the increased resistance level. However, we observed copy number variations
415 in the integron cassette containing the antibiotic resistance genes (Figure 3A). Zooming in on
416 the resistance locus where the *dfrA17* and *sul1* genes are located, we observed substantial
417 CNVs across conditions, replicates and even among clones from the same replicate lineage
418 (Figure 3A, Figure S3). Overall, resistance locus CNVs were highest in clones evolved in
419 isolation, in the well-mixed environment (median 5.2) and in the spatially structured
420 environment (median 3.4). In contrast, copy numbers in *E. coli* evolved in community context
421 were seemingly unaffected across the majority of clones (median 1.7 in the well-mixed and 2.0
422 in the spatially structured environment). Some clones deviated from the trend (Figure S3). The
423 copy number variations (CNVs) of this cassette do not correlate with the MIC (R^2=0.12,

424 *P*=0.13, Figure 3B). Some lineages evolved in isolation in the well-mixed environment had a
425 relatively low MIC despite having higher copy numbers of the antibiotic resistance genes
426 (Figure 3B). This suggests that the MIC is not only influenced by resistance gene copy
427 numbers, but also by other factors.
428 Statistical analysis confirmed that in each evolutionary context the resistance locus CNV
429 differed significantly from the CNV in the well-mixed environment in isolation (Figure S3).
430 This shows that both community presence and environmental structure during evolution
431 influence CNV of antibiotic resistance loci.
432
433 The implications of these data are multifaceted: overall, we found that lineages evolving
434 antibiotic resistance in isolation had higher copy numbers of the *dfrA17-sul1* resistance loci,
435 suggesting selection for increased gene copy numbers during resistance evolution under these
436 conditions. In contrast, lineages evolving in the community context, showed no CNV increase
437 in the majority of replicates and clones (7 out of 10 replicates or 20 out of 30 clones), with only
438 moderate copy number increases in three replicates, indicating a distinct selection regime in
439 the presence of the community. We noted previously that the presence of the community
440 positively affects the growth of *E. coli*. We therefore hypothesize that this community-
441 mediated growth effect increases antibiotic tolerance, and, consequently reduces selection for
442 higher copy numbers of resistance genes for *E. coli* evolved in the presence of the community[57].
443
444 **Environmental and community context modulate genetic adaptation**
445 The number of genomic mutations within the evolved *E. coli* genomes differed significantly
446 between environments. In the well-mixed liquid environment, we detected 25 mutations in total
447 across all clones evolved in isolation, and only 16 mutations in clones evolved in the presence
448 of the community. For the spatially structured environment, we detected in total 45 mutations
449 in clones evolved in isolation, and 48 in clones evolved in the community context (*P*=0.004,
450 *Welch's t*-test comparing the well-mixed and the spatially structured environments). These
451 findings align with our expectations, as a spatially structured environment versus a well-mixed
452 environment is typically associated with diminished selection and increased genetic drift within
453 the population,[58,59] and a lower chance of beneficial mutations sweeping through the
454 population.
455 Because many replicates evolved in the same environment followed parallel phenotypic
456 trajectories (Figure 1AB), we hypothesized that lineages evolving under similar conditions
457 would acquire similar genetic substitutions. To quantify genetic parallelism we calculated the

458 *H-index*,[54] which takes into account the fraction of shared mutations between two isolates on
459 both the gene-level and the Cluster of Orthologous Group (COG) level for substitutions in the
460 *E. coli* chromosome (Figure 4, Materials and Methods). In other work, we have observed quite
461 a high degree of genetic parallelism in replicate populations evolved under the influence of
462 TMP-SMX and bacterial interactions.[15] In contrast, in this study, aside from the CNVs of the
463 resistance genes on the Tn21-like integron cassette, we observed little genomic parallelism,
464 with the exception of replicates evolved in the same spatially structured environment (Figure
465 4A). This indicates that, in the well-mixed environment, genomic mutations were mostly
466 unique to individual replicates (Table S1). An exception involved two *E. coli* replicates evolved
467 in the well-mixed environment in the presence of the community, which shared mutations in
468 one gene. This mutated gene, *folP*, a known target of sulfamethoxazole [46], would allow *E. coli*
469 to tolerate higher antibiotic pressures.[60] The mutations observed, with the exception of *folP*,
470 are, as far as we are aware of, not directly linked to antibiotic resistance to TMP-SMX.[54,60,62]
471 This mutation, in conjunction with other mutations in these replicates, did not result in
472 significant population size differences compared with the other three replicates evolved within
473 the same environment (P>0.05, independent samples t-test with Bonferroni correction). We
474 did not identify any other chromosomal mutations in genes known to confer resistance in the
475 evolved populations (Table S1).
476
477 In replicate lineages that evolved on the spatially structured environment in the presence of the
478 community, two distinct sets of genotypes emerged. Two replicate lineages had an *H-index*
479 value of 0.75, but shared no mutations with the other three replicate lineages evolved under the
480 same conditions. These two replicates harbored mutations in the *treC* gene, a gene involved in
481 the trehalose degradation pathway, converting trehalose-6-phosphate into glucose and glucose-
482 6-phophate. Mutations in this gene point to metabolic adaptation to the nutrients in the
483 environment rather than the antibiotics.[62] The other three replicates evolved in the spatially
484 structured environment in the presence of the community also had an *H-index* of 0.75 for each
485 pairwise comparison, but did not share any mutations with the other two replicate lineages.
486 These three replicate lineages acquired mutations in the *traC, mpl* and *pfkA* genes. The *traC*
487 gene mediates cell-cell contact during conjugation.[63 64] The *traC* mutation in both replicates is
488 a synonymous mutation, suggesting these do not affect functionality, except perhaps through
489 codon bias.[65] The other genes, *mpl and pfkA* and play a role in cell wall biogenesis and
490 carbohydrate degradation, respectively. The *mpL* gene contains a frameshift mutation, likely
491 leading to a loss of function. The gene encodes UDP-N-acetylmuramate, part of the cell-wall

492 recycling machinery.[66] The *pfkA* gene harbored either missense mutations or an in-frame
493 deletion. The gene encodes phosphofructokinase, and is part of the glycolysis pathway. *PfkA*
494 is responsible for about 95% of phosphofructokinase activity in *E. coli.*[67] Disruption of *pfkA*
495 breaks the glycolysis pathway, redirecting fructose 6-phosphate toward alternative pathways
496 such as the pentose phosphate pathway, which is important for the generation of NADPH.[68]
497 One gene that was mutated in all *E. coli* replicates evolved within the spatially structured
498 environment in isolation was *nadR*, a component of the NAD salvage pathway.[69,70] This gene
499 converts β-nicotinamide D-ribonucleotide into diphosphate and NAD^+. The mutations detected
500 were either missense mutations or deletions, likely resulting in loss of function. Inhibition of
501 *nadR* has been shown to increase cellular NAD/NADH levels. Because NADH is an important
502 regulator for enzymes involved in metabolism, these mutations may therefore represent an
503 adaptation to the nutrients conditions rather than to antibiotics.[71] Additionally, elevated levels
504 of NADH have been associated with efflux-mediated antibiotic resistance [71], suggesting a
505 potential indirect contribution to resistance. Four out of five of the replicates also had mutations
506 within the *adhE* gene, which encodes aldehyde-alcohol dehydrogenase.[72] It catalyzes the
507 reaction of acetaldehyde into acetyl-CoA, and also generates NADH. Together, the recurrent
508 mutations in *nadR* and *adhE* point towards selection of NADH-associated metabolic pathways
509 in spatially structured environments, potentially linking metabolic adaptation to antibiotic
510 tolerance.
511
512 Overall, evolution within the spatially structured environments containing TMP-SMX was
513 associated with mutations in genes, *nadR*, *adhE* and *pfkA,* predicted to affect cellular
514 NADH/NADPH levels in *E. coli* in eight out of ten replicates. A previous study has shown that
515 NADPH also contributes to the stabilization of the dihydrofolate reductase-ligand complex,[73]
516 with changes in this complex being signs of trimethoprim resistance. Interestingly, the eight
517 replicates with mutations affecting NAD/NADPH-associated pathways co-occurred with
518 elevated resistance gene copy numbers in lineages evolved in the spatially structured
519 environment (Figure 3A). This suggests that mutations in *nadR, adhE* and *pfkA* may be co-
520 adaptations correlated with increases in resistance gene copy numbers.
521
522 Additionally, mutations within prophages were detected in mutant *E. coli* chromosomes (Table
523 S1). SNPs and complex insertions were observed predominantly in the spatially structured
524 environments. We chose to exclude these from our H-index analysis because prophage regions

525 often evolve at different rates compared to the core bacterial genome and undergo decay after
526 integration[74], and phage activity was not monitored during the evolutionary experiment.
527
528 We observed more evolutionary parallelism at the COG-level, consistent with previous
529 research (Figure 4B).[54,75] Most of the parallelism occurred within replicates evolved in spatially
530 structured environments, both in the presence and absence of the community. In these groups,
531 evolution within the spatially structured environments lead to both parallel genotypic changes
532 (Figure 4) as well as parallel phenotypic adaptation (Figure 1AB). In contrast, lineages evolved
533 in the well-mixed environment, in the presence of the community, showed parallel phenotypic
534 adaptation without corresponding genomic parallelism, contrary to our expectation that
535 stronger selection and larger population sizes would lead to more genetic parallelism.
536 In summary, we observed genetic adaptations at different levels of organization, including the
537 integron cassette harboring resistance genes and mutations in the genomic background underly
538 parallel phenotypic evolutionary trajectories of antibiotic resistance. However, the canalization
539 of antibiotic resistance phenotypes could not be fully explained by genetic substitutions only,
540 highlighting the role of additional factors, including the microbial community. These findings
541 indicate that antibiotic resistance evolution is shaped by multiple levels of genetic of genetic
542 and ecological organization.
543
544 **Conclusion and implications**
545 We observed that the presence of a community has a protective effect on *E. coli* at the onset of
546 the antibiotic resistance evolution experiment, an effect that diminished with increasing
547 antibiotic concentrations. Community presence was associated with a faster evolutionary
548 response in both the well-mixed liquid as well as spatially structured solid environments,
549 consistent with previous findings showing that the presence of other bacteria can speed up and
550 canalize evolutionary trajectories.[15] Phenotypic parallelism was observed across all
551 environmental contexts, either community or environmental structure, except in the well-mixed
552 environment in the absence of the community. In spatially structured environments, the
553 phenotypic parallelism was associated with genetic parallelism. In contrast, in the well-mixed
554 environments, the phenotypic canalization in the presence of the community cannot solely be
555 explained by genetic changes, indicating that non-genetic changes, such as phenotypic
556 plasticity or physiological changes mediated by the community, likely contributed to the
557 evolutionary response to antibiotics.
558

559 The beneficial effect of a community on antibiotic resistance evolution at sub-MIC levels has
560 been observed before.[8,76] Here, we show that the beneficial effect can persist after antibiotic
561 concentrations exceed the initial MIC. Because the AUM environments used in this study are
562 relatively nutrient poor, they likely provide opportunities for positive social interactions among
563 microbes, which may contribute to the sustained beneficial effects observed.[77,78] Theory
564 suggests that communities benefit more from public goods interactions in structured
565 environments, compared to well-mixed environments,[34,35,79,80–82]. However, during the
566 experiment the positive effect of the community on *E.coli* on population size diminished with
567 increasing antibiotic concentrations, over time (Figure 1CD), this was associated with smaller
568 population sizes of the community members.
569
570 In the spatially structured environment, community presence did not have a large impact on
571 the evolved MIC level of *E. coli*. However, the MBC increased when the *E. coli* lineages
572 evolved in isolation were assessed in the presence of the community, indicating that the
573 community-mediated protection remains relevant even for highly resistant lineages (Figure
574 2B). This effect was absent for *E. coli* evolved in the presence of the community in the well-
575 mixed environment. These findings suggest that the beneficial effect of the community is not
576 dependent on the antibiotic concentration alone. Instead, it depends on the evolutionary history
577 of the *E. coli*, particularly whether lineages evolved in a community context. This highlights
578 the importance of the ecological history in shaping antibiotic tolerance and resistance.
579
580 Initial cell density in antibiotic-containing environments is known to influence evolutionary
581 outcomes.[17,76] In both tested environments, *E. coli* reached higher densities when embedded
582 within the community, which was associated with faster evolutionary trajectories towards high
583 antibiotic resistance. This pattern is consistent with the well-known inoculum effect.[16,17]
584 However, for the *E. coli* evolved on the spatial structure in the presence of the community, this
585 did not lead to a higher MIC compared to the *E. coli* evolved in isolation (Figure 1A,B).[8]
586 Because MICs were determined at equal *E.coli* population sizes, this assay does not take into
587 account population size differences during the serial transfer experiments.[16] Nevertheless,
588 population size may indirectly contribute to reaching higher MICs, as the *E. coli* that evolved
589 larger population sizes over 24 hours of growth in the absence of antibiotic reached higher
590 MICs. This suggests that adaptation to the medium-environment contributes to the growth at
591 higher antibiotic concentrations.
592

593 The high degree of copy number variation of the integron cassette carrying the antibiotic
594 resistance genes, both within and across replicates, indicates substantial heterogeneity within
595 replicate populations and suggests a dynamic process in which elevated copy numbers
596 represent a potentially unstable state, likely maintained only under high selective pressure. This
597 interpretation is in line with an insertion sequence-driven amplification mechanism at the
598 resistance locus that can stochastically generate new copies under stress. At the same time,
599 increased CNVs can lead to genomic instability by elevating the probability of disruptive
600 insertions or deleterious homologous recombination events. Such a negative feedback
601 mechanism could promote the continuous generation and purging of excess resistance loci
602 within plasmid lineages.[83] Previous studies have underscored the complexity of plasmid
603 replication and maintenance, suggesting that various factors, including selective pressures and
604 growth rates, can influence the stability of plasmid copy numbers. [84,85,86] The disconnect
605 between resistance gene copy numbers and MICs in our experimental context echoes findings
606 in such systems, where researchers have reported instances of decoupling between plasmid
607 abundance and phenotypic resistance. [87,88] These observations challenge assumptions regarding
608 the straightforward relationship between the presence of antibiotic resistance genes, gene
609 expression and antibiotic resistance. In addition, the mobility of the resistance genes on the
610 integron cassette may further contribute to variation and efficacy of the resistance genes. While
611 our analysis allows us to determine gene copy numbers, it does not resolve the location of
612 individual copies within the plasmid or genome, limiting our ability to predict their functional
613 impact. Because gene expression is influenced by genomic context, including gene location,
614 alignment with regulatory elements, and potential compensatory mutations such as those
615 related to NADH observed in the spatially-structured environment, illustrate the challenges of
616 relying solely on sequence-based approaches in the clinical detection of antimicrobial
617 resistance.
618
619 Together, these findings demonstrate that repeatable antibiotic resistance evolution reflects the
620 combined influence of multiple levels of genetic adaptation, environmental structure and
621 ecological interactions and highlight the need for comprehensive investigations into the
622 multifaceted ecological and genetic interactions governing plasmid-mediated resistance.
623
624
625 **Author contribution**

Conceived and designed the study: LEZ MGJDV. Performed the experiments: LEZ MB JML. Analyzed the data: LEZ TH MGJ. Wrote the manuscript: LEZ JML TH MGJ.

Acknowledgements

LEZ was supported by the Adaptive Life program of the Faculty of Science and Engineering, within GELIFES. MB was supported by the Faculty of Science and Engineering - Adaptive Life PhD Scholarship from the University of Groningen, awarded by GELIFES.

Data

PRJEB90332

637 **References**

638

639 1 Byrd AL, Segre JA. Adapting Koch's postulates: Criteria for disease causation must
640 take microbial interactions into account. *Science (1979)* 2016; **351**: 224–226.

641 2 Peters BM, Jabra-Rizk MA, O'May GA, William Costerton J, Shirtliff ME.
642 Polymicrobial interactions: Impact on pathogenesis and human disease. *Clin Microbiol*
643 *Rev* 2012; **25**: 193–213.

644 3 Gaston JR, Johnson AO, Bair KL, White AN, Armbruster CE. Polymicrobial
645 interactions in the urinary tract: Is the enemy of my enemy my friend? *Infect Immun*
646 2021; **89**. doi:10.1128/IAI.00652-20.

647 4 Zandbergen LE, Halverson T, Brons JK, Wolfe AJ, de Vos MGJ. The Good and the
648 Bad: Ecological Interaction Measurements Between the Urinary Microbiota and
649 Uropathogens. *Front Microbiol* 2021; **12**: 659450.

650 5 Short FL, Murdoch SL, Ryan RP. Polybacterial human disease: The ills of social
651 networking. *Trends Microbiol* 2014; **22**: 508–516.

652 6 Vega NM, Gore J. Collective antibiotic resistance: Mechanisms and implications. *Curr*
653 *Opin Microbiol* 2014; **21**: 28–34.

654 7 Bottery MJ, Pitchford JW, Friman VP. Ecology and evolution of antimicrobial
655 resistance in bacterial communities. *ISME Journal* 2021; **15**: 939–948.

656 8 Klümper U, Recker M, Zhang L, Yin X, Zhang T, Buckling A *et al.* Selection for
657 antimicrobial resistance is reduced when embedded in a natural microbial community.
658 *ISME Journal* 2019; **13**: 2927–2937.

659 9 Algammal A, Hetta HF, Mabrok M, Behzadi P. Editorial: Emerging multidrug-
660 resistant bacterial pathogens "superbugs": A rising public health threat. *Front*
661 *Microbiol* 2023; **14**. doi:10.3389/fmicb.2023.1135614.

662 10 Organization WH. Antimicrobial resistance, Fact sheet N°194,. 2013.

663 11 De Vos MGJ, Zagorski M, McNally A, Bollenbach T. Interaction networks, ecological
664 stability, and collective antibiotic tolerance in polymicrobial infections. *Proc Natl*
665 *Acad Sci U S A* 2017; **114**: 10666–10671.

666 12 Geyrhofer L, Ruelens P, Farr AD, Pesce D, de Visser JAGM, Brenner N. Minimal
667 Surviving Inoculum in Collective Antibiotic Resistance. *mBio* 2023; **14**.
668 doi:10.1128/mbio.02456-22.

669 13 Biswas L, Biswas R, Schlag M, Bertram R, Götz F. Small-colony variant selection as a
670 survival strategy for Staphylococcus aureus in the presence of Pseudomonas
671 aeruginosa. *Appl Environ Microbiol* 2009; **75**: 6910–6912.

672 14 Brauner A, Fridman O, Gefen O, Balaban NQ. Distinguishing between resistance,
673 tolerance and persistence to antibiotic treatment. *Nat Rev Microbiol* 2016; **14**: 320–
674 330.

15 Zandbergen LE, van den Heuvel J, Farr AD, Zwaan BJ, de Visser JAGM, de Vos MGJ. Microbial interactions affect the tempo and mode of antibiotic resistance evolution. *bioRxiv* 2024; : 2024.06.06.597700.

16 Brook I. Inoculum Effect. *Rev Infect Dis* 1989; **11**: 361–368.

17 Tan C, Phillip Smith R, Srimani JK, Riccione KA, Prasada S, Kuehn M *et al.* The inoculum effect and band-pass bacterial response to periodic antibiotic treatment. *Mol Syst Biol* 2012; **8**. doi:10.1038/msb.2012.49.

18 Foster KR, Bell T. Competition, not cooperation, dominates interactions among culturable microbial species. *Current Biology* 2012; **22**: 1845–1850.

19 Hammarlund SP, Harcombe WR. Refining the stress gradient hypothesis in a microbial community. *Proc Natl Acad Sci U S A* 2019; **116**: 15760–15762.

20 Piccardi P, Vessman B, Mitri S. Toxicity drives facilitation between 4 bacterial species. *Proc Natl Acad Sci U S A* 2019; **116**: 15979–15984.

21 Lee J-H, Lee J. Indole as an intercellular signal in microbial communities. *FEMS Microbiol Rev* 2010; **34**: 426–444.

22 Vos MGJ de, Jansen V, Bouhlali O, Vlasblom A, Zandbergen LE, Windt I van der *et al.* Pyocyanin produced by Pseudomonas aeruginosa Creates Legacy Effects That Boost Antibiotic Resistance Evolution in Enterococci. *bioRxiv* 2025; : 2025.12.04.692361.

23 Flemming HC, Wingender J, Szewzyk U, Steinberg P, Rice SA, Kjelleberg S. Biofilms: An emergent form of bacterial life. *Nat Rev Microbiol* 2016; **14**: 563–575.

24 Costerton JW, Stewart PS, Greenberg. Bacterial biofilms: a common cause of persistant infections. *Science (1979)* 1999; **284**: 1318–1322.

25 Dieckmann U, Law R, Metz JAJ. *The Geometry of Ecological Interactions: Simplifying Spatial Complexity*. Cambridge University Press, 2002 doi:10.1016/s0925-8574(01)00102-1.

26 Tilman D, Kareiva P. *Spatial Ecology: The Role of Space in Population Dynamics and Interspecific Interactions. David Tilman , Peter Kareiva*. Princeton University Press, 1998 doi:10.1086/420507.

27 Johnson CR, Seinen I. Selection for restraint in competitive ability in spatial competition systems. *Proceedings of the Royal Society B: Biological Sciences* 2002; **269**: 655–663.

28 Kerr B, Riley MA, Feldman MW, Bohannan BJM. Local dispersal promotes biodiversity in a real-life game of rock-paper-scissors. *Nature* 2002; **418**: 171–174.

29 Yanni D, Márquez-Zacarías P, Yunker PJ, Ratcliff WC. Drivers of Spatial Structure in Social Microbial Communities. *Current Biology* 2019; **29**: R545–R550.

30 Evans KC, Benomar S, Camuy-Vélez LA, Nasseri EB, Wang X, Neuenswander B *et al.* Quorum-sensing control of antibiotic resistance stabilizes cooperation in *Chromobacterium violaceum*. *ISME J* 2018; **12**: 1263–1272.

714 31 Chuang SK, Vrla GD, Fröhlich KS, Gitai Z. Surface association sensitizes
715 Pseudomonas aeruginosa to quorum sensing. *Nat Commun* 2019; **10**: 4118.

716 32 Nowak MA, May RM. Evolutionary games and spatial chaos. *Nature* 1992; **359**: 826–
717 829.

718 33 Santos FC, Pacheco JM, Lenaerts T. Evolutionary dynamics of social dilemmas in
719 structured heterogeneous populations. *Proc Natl Acad Sci U S A* 2006; **103**: 3490–
720 3494.

721 34 Nadell CD, Drescher K, Foster KR. Spatial structure, cooperation and competition in
722 biofilms. Nat. Rev. Microbiol. 2016; **14**: 589–600.

723 35 Verbruggen E, El Mouden C, Jansa J, Akkermans G, Bücking H, West SA *et al.*
724 Spatial structure and interspecific cooperation: Theory and an empirical test using the
725 mycorrhizal mutualism. *American Naturalist* 2012; **179**: E133-46.

726 36 Habets MGJL, Rozen DE, Hoekstra RF, De Visser JAGM. The effect of population
727 structure on the adaptive radiation of microbial populations evolving in spatially
728 structured environments. *Ecol Lett* 2006; **9**: 1041–1048.

729 37 Perfeito L, Pereira MI, Campos PR, Gordo I. The effect of spatial structure on
730 adaptation in Escherichia coli. *Biol Lett* 2008; **4**: 57–59.

731 38 Bailey SF, Trudeau A, Tulowiecki K, McGrath M, Belle A, Fountain H *et al.* Spatial
732 structure affects evolutionary dynamics and drives genomic diversity in experimental
733 populations of *Pseudomonas fluorescens*. 2021. doi:10.1101/2021.09.28.461808.

734 39 Momeni B, Waite AJ, Shou W. Spatial self-organization favors heterotypic
735 cooperation over cheating. *Elife* 2013; **2**. doi:10.7554/eLife.00960.

736 40 Lobanov A, Dyckman S, Kurkjian H, Momeni B. Spatial structure favors microbial
737 coexistence except when slower mediator diffusion weakens interactions. *Elife* 2023;
738 **12**. doi:10.7554/eLife.82504.

739 41 Bustamante M, Mei S, Daras IM, van Doorn GS, Falcao Salles J, de Vos MGJ. An
740 eco-evolutionary perspective on antimicrobial resistance in the context of One Health.
741 *iScience* 2025; **28**: 111534.

742 42 Bustamante M, Koopman F, Martens J, Brons JK, DelaFuente J, Hackl T *et al.*
743 Community context influences the conjugation efficiency of Escherichia coli. *FEMS*
744 *Microbes* 2024; **5**. doi:10.1093/FEMSMC/XTAE023.

745 43 Sünderhauf D, Klümper U, Gaze WH, Westra ER, van Houte S. Interspecific
746 competition can drive plasmid loss from a focal species in a microbial community.
747 *ISME Journal* 2023; **17**: 1765–1773.

748 44 Stalder T, Top E. Plasmid transfer in biofilms: a perspective on limitations and
749 opportunities. *NPJ Biofilms Microbiomes* 2016; **2**: 16022.

750 45 Croxall G, Weston V, Joseph S, Manning G, Cheetham P, McNally A. Increased
751 human pathogenic potential of Escherichia coli from polymicrobial urinary tract

752 infections in comparison to isolates from monomicrobial culture samples. *J Med*
753 *Microbiol* 2011; **60**: 102–109.

754 46 Hitchings GH. Mechanism of action of trimethoprim-sulfamethoxazole--I. *J Infect Dis*
755 1973; **128**: S433.

756 47 Kolmogorov M, Yuan J, Lin Y, Pevzner PA. Assembly of long, error-prone reads
757 using repeat graphs. *Nat Biotechnol* 2019; **37**: 540–546.

758 48 Zimin A V., Puiu D, Luo M-C, Zhu T, Koren S, Marçais G *et al.* Hybrid assembly of
759 the large and highly repetitive genome of *Aegilops tauschii* , a progenitor of bread
760 wheat, with the MaSuRCA mega-reads algorithm. *Genome Res* 2017; **27**: 787–792.

761 49 Schwengers O, Jelonek L, Dieckmann MA, Beyvers S, Blom J, Goesmann A. Bakta:
762 rapid and standardized annotation of bacterial genomes via alignment-free sequence
763 identification. *Microb Genom* 2021; **7**. doi:10.1099/mgen.0.000685.

764 50 Camargo AP, Roux S, Schulz F, Babinski M, Xu Y, Hu B *et al.* Identification of
765 mobile genetic elements with geNomad. *Nat Biotechnol* 2024; **42**: 1303–1312.

766 51 Li H. Minimap2: pairwise alignment for nucleotide sequences. *Bioinformatics* 2018;
767 **34**: 3094–3100.

768 52 Garrison E, Marth G. Haplotype-based variant detection from short-read sequencing.
769 2012.

770 53 Danecek P, Bonfield JK, Liddle J, Marshall J, Ohan V, Pollard MO *et al.* Twelve years
771 of SAMtools and BCFtools. *Gigascience* 2021; **10**. doi:10.1093/gigascience/giab008.

772 54 Schenk MF, Zwart MP, Hwang S, Ruelens P, Severing E, Krug J *et al.* Population size
773 mediates the contribution of high-rate and large-benefit mutations to parallel evolution.
774 Nat. Ecol. Evol. 2022; **6**: 439–447.

775 55 Mann R, Mediati DG, Duggin IG, Harry EJ, Bottomley AL. Metabolic adaptations of
776 Uropathogenic E. coli in the urinary tract. *Front Cell Infect Microbiol* 2017; **7**.
777 doi:10.3389/fcimb.2017.00241.

778 56 Liebert CA, Hall RM, Summers AO. Transposon Tn 21 , Flagship of the Floating
779 Genome . *Microbiology and Molecular Biology Reviews* 1999; **63**: 507–522.

780 57 Klümper U, Recker M, Zhang L, Yin X, Zhang T, Buckling A *et al.* Selection for
781 antimicrobial resistance is reduced when embedded in a natural microbial community.
782 *The ISME Journal 2019 13:12* 2019; **13**: 2927–2937.

783 58 Zhang Q, Lambert G, Liao D, Kim H, Robin K, Tung CK *et al.* Acceleration of
784 emergence of bacterial antibiotic resistance in connected microenvironments. *Science*
785 *(1979)* 2011; **333**: 1764–1767.

786 59 Hallatschek O, Hersen P, Ramanathan S, Nelson DR. Genetic drift at expanding
787 frontiers promotes gene segregation. *Proceedings of the National Academy of Sciences*
788 2007; **104**: 19926–19930.

789 60 Buwembo W, Aery S, Rwenyonyi CM, Swedberg G, Kironde F. Point mutations in the
790 folP gene partly explain sulfonamide resistance of streptococcus mutans. *Int J*
791 *Microbiol* 2013; **2013**: 367021.

792 61 Rimmele M, Boos W. Trehalose-6-phosphate hydrolase of Escherichia coli. *J*
793 *Bacteriol* 1994; **176**: 5654–5664.

794 62 Botelho J, Schulenburg H. The Role of Integrative and Conjugative Elements in
795 Antibiotic Resistance Evolution. *Trends Microbiol* 2021; **29**: 8–18.

796 63 Amro J, Baron C. TraC of the conjugative plasmid pKM101 is secreted as a monomer
797 in outer membrane vesicles and stimulates conjugation. *bioRxiv* 2022; : 2022–2027.

798 64 Parvathy ST, Udayasuriyan V, Bhadana V. Codon usage bias. *Mol Biol Rep* 2022; **49**:
799 539–565.

800 65 Mengin-Lecreulx D, van Heijenoort J, Park JT. Identification of the mpl gene
801 encoding UDP-N-acetylmuramate: L-alanyl-gamma-D-glutamyl-meso-
802 diaminopimelate ligase in Escherichia coli and its role in recycling of cell wall
803 peptidoglycan. *J Bacteriol* 1996; **178**: 5347–5352.

804 66 Vinopal RT, Clifton D, Fraenkel DG. PfkA locus of Escherichia coli. *J Bacteriol* 1975;
805 **122**: 1162–1171.

806 67 Siedler S, Bringer S, Bott M. Increased NADPH availability in Escherichia coli:
807 improvement of the product per glucose ratio in reductive whole-cell
808 biotransformation. *Appl Microbiol Biotechnol* 2011; **92**: 929–937.

809 68 Gerasimova, Gelfand. Evolution of the nadr regulon in enterobacteriaceae. *J Bioinform*
810 *Comput Biol* 2005; **03**: 1007–1019.

811 69 Tritz GJ, Chandler JL. Recognition of a Gene Involved in the Regulation of
812 Nicotinamide Adenine Dinucleotide Biosynthesis. *J Bacteriol* 1973; **114**: 128–136.

813 70 Arce-Rodríguez A, Pankratz D, Preusse M, Nikel PI, Häussler S. Dual Effect: High
814 NADH Levels Contribute to Efflux-Mediated Antibiotic Resistance but Drive
815 Lethality Mediated by Reactive Oxygen Species. *mBio* 2022; **13**.
816 doi:10.1128/mbio.02434-21.

817 71 Kessler D, Leibrecht I, Knappe J. Pyruvate-formate-lyase-deactivase and acetyl-CoA
818 reductase activities of *Escherichia coli* reside on a polymeric protein particle encoded
819 by *adhE*. *FEBS Lett* 1991; **281**: 59–63.

820 72 Krucinska J, Lombardo MN, Erlandsen H, Estrada A, Si D, Viswanathan K *et al.*
821 Structure-guided functional studies of plasmid-encoded dihydrofolate reductases
822 reveal a common mechanism of trimethoprim resistance in Gram-negative pathogens.
823 *Commun Biol* 2022; **5**: 459.

824 73 Canchaya C, Proux C, Fournous G, Bruttin A, Brüssow H. Prophage genomics.
825 *Microbiol Mol Biol Rev* 2003; **67**: 238–76, table of contents.

826 74 Tenaillon O, Rodríguez-Verdugo A, Gaut RL, McDonald P, Bennett AF, Long AD *et*
827 *al.* The molecular diversity of adaptive convergence. *Science (1979)* 2012; **335**: 457–
828 461.

829 75 Yurtsev EA, Chao HX, Datta MS, Artemova T, Gore J. Bacterial cheating drives the
830 population dynamics of cooperative antibiotic resistance plasmids. *Mol Syst Biol* 2013;
831 **9**: 683.

832 76 Piccardi P, Vessman B, Mitri S. Toxicity drives facilitation between 4 bacterial
833 species. *Proceedings of the National Academy of Sciences* 2019; **116**: 15979–15984.

834 77 Adamowicz EM, Muza M, Chacón JM, Harcombe WR. Cross-feeding modulates the
835 rate and mechanism of antibiotic resistance evolution in a model microbial community
836 of Escherichia coli and Salmonella enterica. *PLoS Pathog* 2020; **16**: e1008700.

837 78 Brockhurst MA, Habets MGJL, Libberton B, Buckling A, Gardner A. Ecological
838 drivers of the evolution of public-goods cooperation in bacteria. *Ecology* 2010; **91**:
839 334–340.

840 79 Keogh D, Tay WH, Ho YY, Dale JL, Chen S, Umashankar S *et al.* Enterococcal
841 Metabolite Cues Facilitate Interspecies Niche Modulation and Polymicrobial Infection.
842 *Cell Host Microbe* 2016; **20**: 493–503.

843 80 Co AD, van Vliet S, Kiviet DJ, Schlegel S, Ackermann M. Short-range interactions
844 govern the dynamics and functions of microbial communities. *Nat Ecol Evol* 2020; **4**:
845 366–375.

846 81 van Tatenhove-Pel RJ, Rijavec T, Lapanje A, van Swam I, Zwering E, Hernandez-
847 Valdes JA *et al.* Microbial competition reduces metabolic interaction distances to the
848 low µm-range. *ISME Journal* 2021; **15**: 688–701.

849 82 Dimitriu T, Matthews AC, Buckling A. Increased copy number couples the evolution
850 of plasmid horizontal transmission and plasmid-encoded antibiotic resistance. *Proc*
851 *Natl Acad Sci U S A* 2021; **118**: e2107818118.

852 83 Baltrus DA. Exploring the costs of horizontal gene transfer. *Trends Ecol Evol* 2013;
853 **28**: 489–495.

854 84 Millan AS, Santos-Lopez A, Ortega-Huedo R, Bernabe-Balas C, Kennedy SP,
855 Gonzalez-Zorn B. Small-plasmid-mediated antibiotic resistance is enhanced by
856 increases in plasmid copy number and bacterial fitness. *Antimicrob Agents Chemother*
857 2015; **59**: 3335–3341.

858 85 San Millan A, MacLean RC. Fitness Costs of Plasmids: a Limit to Plasmid
859 Transmission. *Microbiol Spectr* 2017; **5**. doi:10.1128/microbiolspec.mtbp-0016-2017.

860 86 Bouma JE, Lenski RE. Evolution of a bacteria/plasmid association. *Nature* 1988; **335**:
861 351–352.

862 87 Stokes HW, Gillings MR. Gene flow, mobile genetic elements and the recruitment of
863 antibiotic resistance genes into Gram-negative pathogens. *FEMS Microbiol Rev* 2011;
864 **35**: 790–819.

865

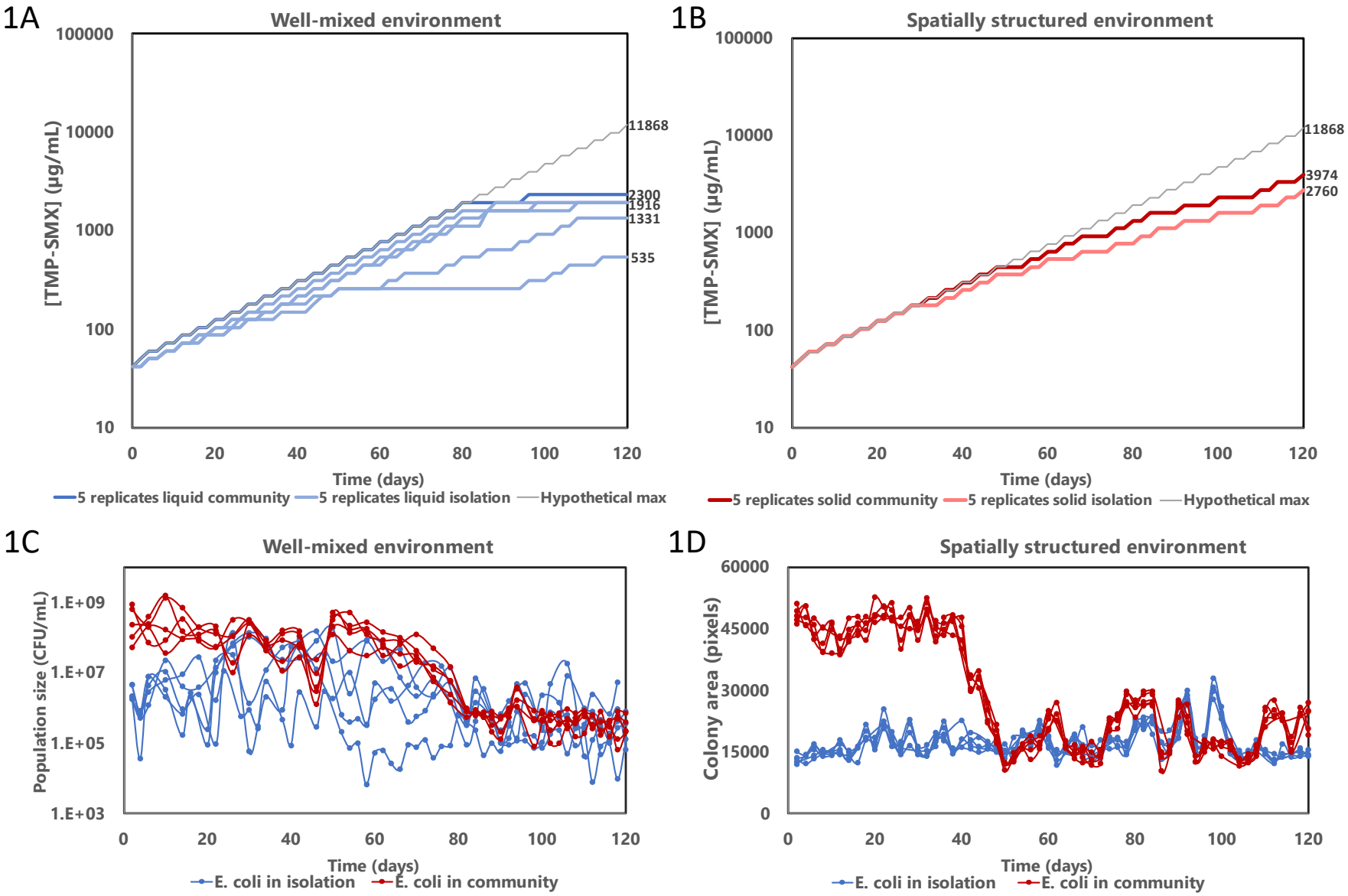
1A
Well-mixed environment
[TMP-SMX] (µg/mL)
100000
10000
1000
100
10
0
20
40
60
80
100
120
Time (days)
11868
2300
1916
1331
535
5 replicates liquid community
5 replicates liquid isolation
Hypothetical max
1B
Spatially structured environment
[TMP-SMX] (µg/mL)
100000
10000
1000
100
10
0
20
40
60
80
100
120
Time (days)
11868
3974
2760
5 replicates solid community
5 replicates solid isolation
Hypothetical max
1C
Well-mixed environment
Population size (CFU/mL)
1.E+09
1.E+07
1.E+05
1.E+03
0
20
40
60
80
100
120
Time (days)
E. coli in isolation
E. coli in community
1D
Spatially structured environment
Colony area (pixels)
60000
45000
30000
15000
0
0
20
40
60
80
100
120
Time (days)
E. coli in isolation
E. coli in community

Figure 1 | Phentoypic trajectories of trimethoprim-sulfamethoxazole antibiotic resistance evolution and population sizes of *E. coli* over time. *E. coli* evolved in the presence and absence of a community, consisting of *Klebsiella pneumoniae*, *Enterococcus faecium* and *Staphylococcus epidermidis*. *E. coli* was evolved in presence of trimethoprim-sulfamethoxazole (TMP-SMX) at a 1:5 ratio. Each condition was replicated five times. **AB,** concentration of TMP-SMX in the medium for all evolving replicate lineages within the well-mixed liquid environment (A) and spatially structured environment (B) over time. Concentrations of TMP-SMX are given by the trimethoprim concentrations. All five replicate lineages converged and overlapped for *E. coli* evolving in the presence of the community, for both well-mixed spatially structured environments. Different trajectories can be observed for *E. coli* evolving in the absence of the community within the well-mixed liquid environment. **C,** population size of *E. coli* in the well-mixed liquid environment in CFU/mL. A decline of the *E. coli* population size evolved in the presence of the community can be observed after forty eight days, for all five replicate lineages. The population size of *E. coli* evolving in isolation showed large fluctuations in the first eighty days, these became less diverse after this time. **D,** population size of *E. coli* evolved in the spatially structured solid environment measured as colony area in pixels. A clear decline of colony size for *E. coli* evolved in the presence of the community can be observed after roughly forty days for all five replicate lineages.

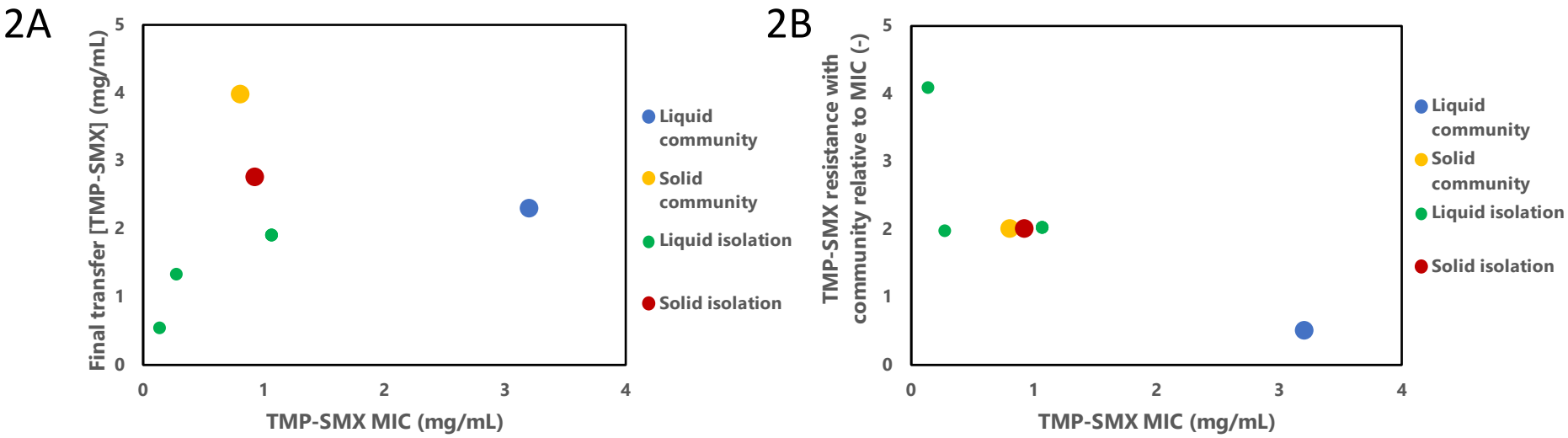

Figure 2 | Relationship between the minimal inhibitory concentration (MIC) of evolved clones, in the presence and absence of the community, and the antibiotic concentrations at final transfer. The size of the data points shows the number of replicates, with the smallest data point being one replicate and the largest all five replicates. *E. coli* was evolved in presence of trimethoprim-sulfamethoxazole (TMP-SMX) at a 1:5 ratio. Concentrations of TMP-SMX are given by the trimethoprim concentrations. **A,** MIC of evolved *E.coli* versus the concentration of antibiotic at the final transfer step at day 120. No clear correlation between the MIC of evolved clones, and the concentration of antibiotic in the medium at their final transfer could be observed. **B,** MIC of evolved *E.coli* versus the community effect on MIC. The community resistance effect was determined by performing an MBC assay in the presence of the community, followed by subsequent transfer on agar. The concentration of trimethoprim-sulfamethoxazole at which no *E. coli* could be observed on the agar, is given relative to the MBC of *E. coli* in isolation. Therefore, a value above 1 on the y-axis indicates a higher observed resistance compared to measured MIC, while a value below 1 indicates a low resistance compared to the MIC. Only *E. coli* evolved in liquid medium in the presence of the community did not benefit from the presence of the community in the community MBC assay (blue). Absolute resistance levels in the presence of community are depicted in Figure S1.

3A

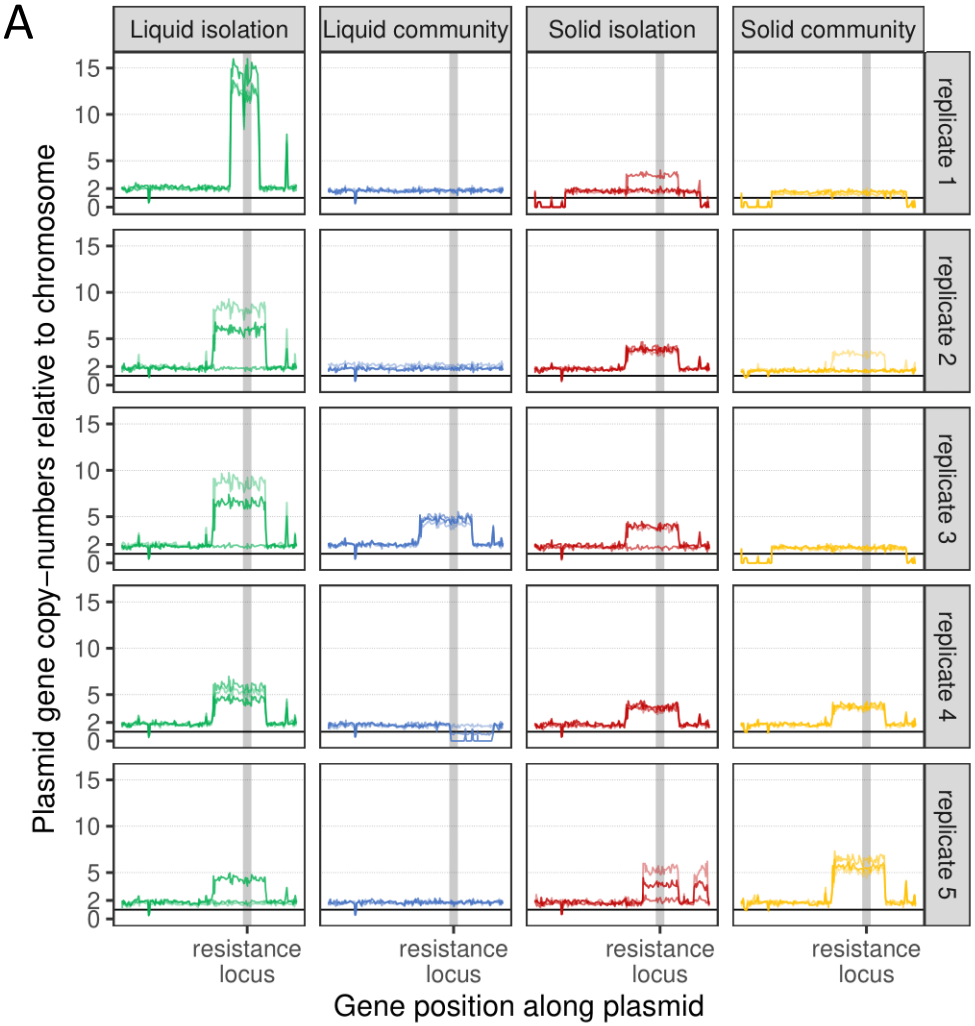
Liquid isolation
Liquid community
Solid isolation
Solid community
replicate 1
replicate 2
replicate 3
replicate 4
replicate 5
Plasmid gene copy−numbers relative to chromosome
15
10
5
2
0
resistance locus
Gene position along plasmid

3B

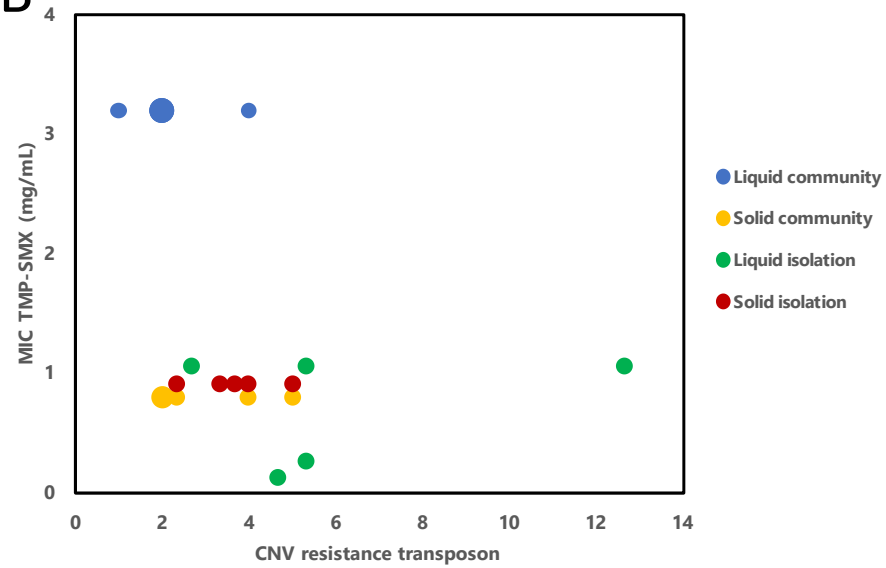
MIC TMP-SMX (mg/mL)
CNV resistance transposon
0
1
2
3
4
0
2
4
6
8
10
12
14
Liquid community
Solid community
Liquid isolation
Solid isolation

Figure 3 | Copy number variation in the plasmid containing the antibiotic resistance genes in the final transfer mutants. Three clones were sequenced per replicate, showing genetic copy number variation within the population. **A.** Copy number variation in the TN21-like integron cassette part of the plasmid containing *dfrA17* and *sul1,* which confer resistance to trimethoprim and sulfamethoxazole, respectively, in each of the sequenced clones. The highlighted region in gray contains the resistance genes, showing overall a tendency for increased copy numbers of this region. Some replicates do not have increased copy numbers of the resistance genes compared to the wild type, particularly those evolved in the liquid environment in the presence of the community (blue), and in the solid spatially structured environment in the presence of the community (yellow). **B.** Average copy number variation per replicate in the TN21-like integron cassette part of the plasmid containing *dfrA17* and *sul1* resistance genes versus resistance level (MIC) of evolved replicate lineages. Concentrations of trimethoprim-sulfamethoxazole (1:5 ratio) are given by the trimethoprim concentrations. No clear pattern between replicates evolved in the same environment could be observed. Copy number variation for each sequenced clone is depicted in Figure S3.

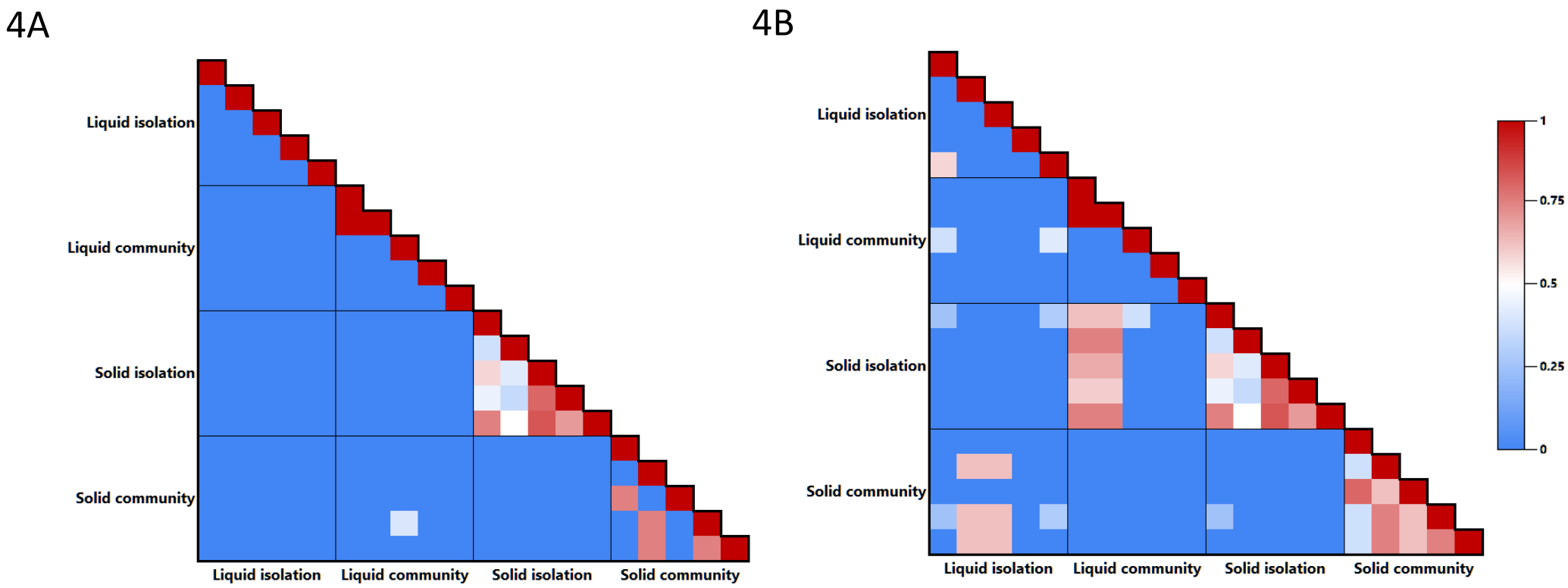

Figure 4 | Clustering and mutation repeatability of final replicates clustered on gene and COG level. The level of genetic parallelism in evolved clones is given by the *H*-index. Higher *H*-index values indicate a higher parallelism of the two genotypes compared. Three clones per replicate were sequenced per environment. Comparisons in the blocks around the diagonal in each figure show the intra-environment comparisons, while the other blocks show the inter-environment comparisons. Solid indicates the spatially structured environment and liquid indicates the well-mixed environment. Mutations and genes are shown in Supplementary table 1. **A,** *H*-index of mutation repeatability at the gene-level of *E. coli* mutants. Within the spatially structured environment there was some repeated evolution, while very few replicates within the well-mixed liquid environment showed repeated evolution. **B,** *H*-index of mutation repeatability at the COG-level. Most genetic parallelism is found in the spatially-structured environment.